Appl. Phys. A 84, 271–276 (2006)
DOI: 10.1007/s00339-006-3617-x

Applied Physics A
Materials Science & Processing

A.S. FERLAUTO[1,✉]
D.Z. DE FLORIO[2]
F.C. FONSECA[3]
V. ESPOSITO[4]
R. MUCCILLO[3]
E. TRAVERSA[4]
L.O. LADEIRA[1]

Chemical vapor deposition of multi-walled carbon nanotubes from nickel/yttria-stabilized zirconia catalysts

[1] Departamento de Física, Universidade Federal de Minas Gerais, Av. Antônio Carlos 6627, 31270-901 Belo Horizonte, MG, Brazil
[2] Instituto de Química, UNESP, R. Prof. Francisco Degni, 14801-970 Araraquara, SP, Brazil
[3] Instituto de Pesquisas Energéticas e Nucleares, Travessa R 400, 05508-170 São Paulo, SP, Brazil
[4] Dipartimento di Scienze e Tecnologie Chimiche, Università di Roma "Tor Vergata", Via della Ricerca Scientifica, 00133 Rome, Italy

Received: 24 November 2005/Accepted: 22 April 2006
Published online: 2 June 2006 •

ABSTRACT Multi-walled carbon nanotubes (MWNT) were produced by chemical vapor deposition using yttria-stabilized zirconia/nickel (YSZ/Ni) catalysts. The catalysts were obtained by a liquid mixture technique that resulted in fine dispersed nanoparticles of NiO supported in the YSZ matrix. High quality MWNT having smooth walls, few defects, and low amounts of by-products such as amorphous carbon were obtained, even from catalysts with large Ni concentrations (> 50 wt. %). By adjusting the experimental parameters, such as flux of the carbon precursor (ethylene) and Ni concentration, both the MWNT morphology and the process yield could be controlled. The resulting YSZ/Ni/MWNT composites can be interesting due to their mixed ionic-electronic transport properties, which could be useful in electrochemical applications.

PACS 61.46.Fg; 81.15.Gh; 82.45.Jn

1 Introduction

Carbon nanotubes (CNTs) have been the focus of intense research in recent years. Numerous studies focusing on their diverse properties have been performed and several applications have been proposed (for a recent review see [1]). Among the different preparation techniques, chemical vapor deposition (CVD) methods are being investigated as the most promising alternative for both the large scale and the controlled production of CNTs [2]. In these methods, CNTs are formed from the pyrolysis of hydrocarbon gases (or other C containing gases), which is catalyzed by the presence of nano-sized particles of transition metals such as Fe, Ni, and Co. The metal catalysts can be supplied in the form of nanoparticles [3], as thin films over substrates [4], directly from the vapor of metallocene molecules [5], or embedded in a supportive matrix [6–10]. In the last case, several combinations of metal catalysts and support materials have been investigated [11]; however, most of the studies have been limited to oxide supports such as Al_2O_3 [8], SiO_2 [7], MgO [6, 10], and zeolites [9]. These are chosen because mesoporous powders of these materials are readily available, and their characteristics of large surface area and small pore dimensions are believed to provide a good support for the anchoring of nano-sized metal particles [11]. Nevertheless, metal oxides that are ionic conductors such as yttria-stabilized zirconia (ZrO_2:8 mol % Y_2O_3) have been largely ignored as catalyst support for CNT grown. Besides, metal concentration in the catalysts is in general kept relatively low ($\leq$ 15 wt. %), in order to avoid the coarsening of the metallic particles, which inhibit CNT growth and promote amorphous carbon formation [11]. In general, the goal of CVD production by using supported catalysts is to generate large amounts of CNTs that subsequently can be purified by removing the catalyst support and metals, and then be studied or used in some application. Conversely, there have been only few studies on the different properties of as-grown oxide/metal/CNT composites, most of them focusing on their mechanical properties [12].

In a previous work, we have developed a liquid mixture route to prepare yttria-stabilized zirconia/nickel oxide (YSZ/NiO) powders in a wide range of NiO concentration, consisting of finely dispersed NiO particles over highly dense YSZ particles [13]. It was shown that the resulting composite is an excellent starting material for electrochemical applications such as gas separation membranes and anodes of solid oxide fuel cell (SOFC) [14–16]. In particular, the YSZ/Ni composite, with Ni content above the percolation value for electronic transport, is the most commonly used material in SOFC anodes [15, 16]. The obtained characteristic of good dispersion of NiO nanoparticles in the YSZ matrix has motivated us to study the performance of such materials as catalyst for CNT growth by CVD. There have been only few reports on the utilization of zirconium oxide as catalyst support for CNT fabrication by the decomposition of methane [17, 18]. ZrO_2 nanoparticles have also been deposited over oxidized silicon substrates and used as spacer to prevent iron oxide nanoparticles from agglomeration in CNT preparation [19]. On the other hand, the formation of CNTs as an undesired by-product (coke) of hydrocarbon reform by using similar catalysts is commonly observed [20]. In the present work, we present a systematic study focused on the controlled CVD production of multi-wall carbon nanotubes (MWNT) by using YSZ/Ni catalysts having a wide range of Ni concentration. The MWNT morphology and the process yield can be controlled by adjusting the Ni concentration in the catalyst and CVD parameters such as gas flow. The resulting as-grown YSZ/Ni/MWNT composites can be envisioned as

✉ Fax: +55-31-3499.5600, E-mail: aferlauto@gmail.com

potential components of electrochemical devices due to their mixed ionic-electronic transport properties. The proposed direct route for this composite production has important advantages over commonly used mixing procedures of the different materials. The direct route eliminates the steps of CNT purification and dispersion, while ensuring an enhanced phase distribution and homogeneity.

2 Experimental

The YSZ/NiO powders were prepared by a liquid mixture technique described in details elsewhere [13]. Briefly, a mixture of YSZ (Tosoh) and nickel acetate tetrahydrate (Carlo Erba) was dissolved in ethanol. The solution was dispersed in an ultrasonic bath for approximately 1 h and then heated on a hot plate at 80 °C under vigorous stirring to promote the rapid evaporation of the ethanol. The obtained powder was calcined at 450 °C. The initial NiO content was tailored to obtain after NiO reduction, three different Ni concentrations (v), $v = 7$, 37, and 55 wt. %. The first value (7 wt. %) is within the range commonly used in metal-supported catalysts for CNT growth [6–10], whereas the two higher values correspond approximately to the lower (37 wt. %) and higher (55 wt. %) limits for mixed ionic-electronic conduction in YSZ/Ni composites [14, 21].

The CVD was performed in a horizontal furnace (2-inch quartz tube) at atmospheric pressure by using conditions usually employed for the production of MWNT [11]. Typically, 20–80 mg of the catalyst powder was loaded in the reactor, which was heated to 700 °C under Ar flow (1000 sccm). A pretreatment, 30 min under H_2-flow (500 sccm), was performed in order to reduce the NiO. Next, to promote CNT growth, a mix of ethylene (C_2H_4), H_2 and Ar was added, resulting in gas mixture of $[C_2H_4] : [H_2] : [Ar]$ of $(10 - 35) : 500 : 1000$ (values in sccm). The low concentration of C_2H_4 in the gas mixture is selected to avoid its gas-phase decomposition that would lead to the formation of large amounts amorphous carbon.

Phase analyses were performed in the catalyst powder and in the as-grown materials by X-ray diffraction (XRD - Bruker AXS D8 Advance diffractometer) in a Bragg–Brentano configuration using CuKα radiation in the $20° \leq 2\theta \leq 70°$ range. The morphology of the catalyst powders were analyzed by field emission scanning electron microscopy (FE-SEM, LEO model 1530). The as-grown YSZ/Ni/MWNT materials were analyzed by standard SEM (JEOL 840A) and transmission electron microscopy (TEM JEOL 200C). The YSZ/Ni/MWNT composites were also analyzed by thermogravimetric analysis (TGA - Netzsch STA 409E), by collecting curves for temperatures up to 1000 °C (10 °C/min heating and cooling rates) under a flow of synthetic air or nitrogen.

3 Results and discussion

The liquid mixture route used for the preparation of the YSZ/NiO powders was found to result in materials with optimized microstructure and transport properties for electrochemical applications [13, 14]. The microstructure of such powders consists of a homogeneous mixture of finely dispersed NiO particles over the YSZ matrix. It was observed that this microstructure is mostly independent of the NiO concentration, even for large concentrations. As an example, Fig. 1 depicts representative XRD (a) and FEG-SEM results (b) of a YSZ/NiO powder with $v = 37\%$. Figure 1a shows that only the peaks corresponding to YSZ and NiO phases are present in the XRD diffraction patterns, and analysis of the NiO peaks by the Scherrer formula reveals that the NiO crystallite sizes is ~ 7 nm. FE-SEM images confirmed that the NiO nanoparticles have a diameter of $d_{NiO} \sim 5$–10 nm and are well distributed over the surface of the larger YSZ particles ($d_{YSZ} \sim 100$ nm), as shown in Fig. 1b.

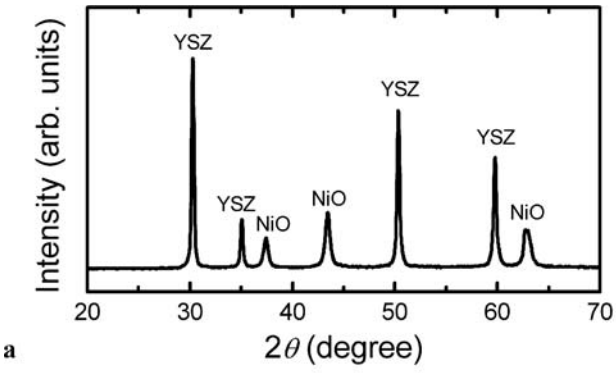

a

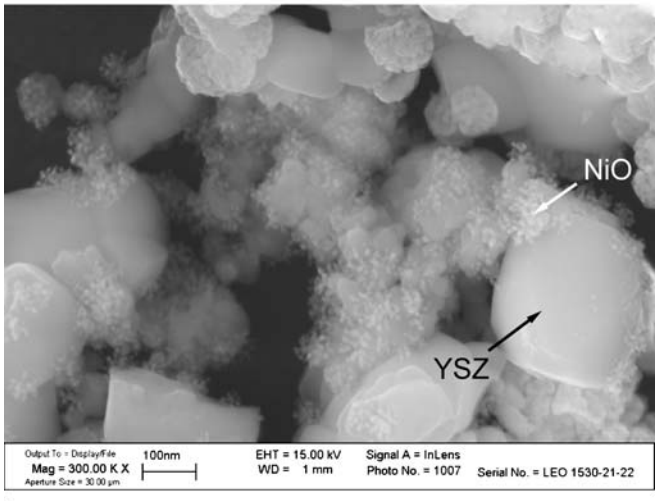

b

FIGURE 1 (**a**) XRD pattern and (**b**) FE-SEM micrograph of the YSZ/NiO catalyst powder with Ni concentration, $v = 37$ wt. %. In (**b**), NiO particles ($d \sim 5$–10 nm) well-dispersed over the YSZ particles ($d \sim 100$ nm) are clearly discerned. The two phases, NiO and YSZ, are identified by the *arrows*

Based on these results, we have decided to study the performance of such composites as catalyst for CNT growth by CVD. We have chosen to fix the process temperature and duration at 700 °C and 30 min, respectively, and perform a systematic investigation of the effects of the Ni concentration in the catalyst powder (v) and the C_2H_4 flux (φ) on the resulting CNT morphology and process efficiency. Figure 2a–c displays SEM images of as-grown CNT materials prepared with $\varphi = 10$ sccm that illustrate the effect of the Ni concentration. Dense mats of filamentary structures are observed in the SEM images for all studied v, and catalyst particles are hardly detected, being mostly hidden within such mats. There exists a significant dependence of the morphology of the produced materials on the Ni concentration. For $v = 7$ wt. % (Fig. 2a), there is a predominance of curly CNTs

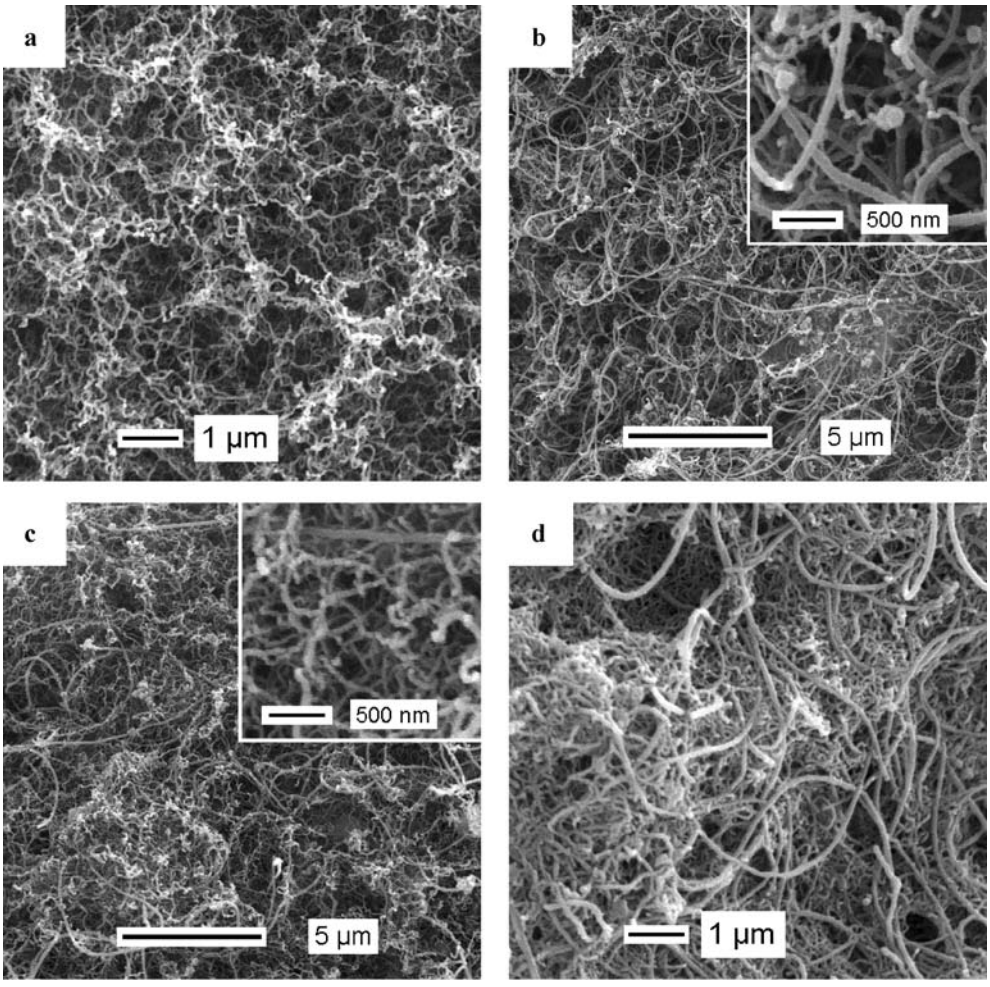

FIGURE 2 SEM micrographs of the as-grown CNT-materials prepared from catalysts with different Ni concentration (v), and by using different ethylene flux (φ): (**a**) $v = 7$ wt. %, $\varphi = 10$ sccm, (**b**) $v = 37$ wt. %, $\varphi = 10$ sccm, (**c**) $v = 55$ wt. %, $\varphi = 10$ sccm, and (**d**) $v = 37$ wt. %, $\varphi = 35$ sccm. The *insets* in (**b**) and (**c**) show higher magnification micrographs

of small diameter, whereas for $v = 37$ wt. % (Fig. 2b), the CNTs are less curly and much longer and thicker. Interestingly, for $v = 55$ wt. % (Fig. 2c), the resulting material seems to be a mixture of small curly filaments, similar to those observed in Fig. 2a, and longer, thicker filaments, similar to those observed in Fig. 2b. Figure 2d illustrates the effect of the C_2H_4 flux for materials prepared using the catalyst powder with $v = 37$ wt. %. It is observed that, when the flux is increased from 10 sccm (Fig. 2b) to 35 sccm (Fig. 2d), there is a significant increase in the amount of the produced CNT. Denser mats of CNTs are formed that completely cover the whole image and hide the catalyst particles. Again, two distinct CNT morphologies can be distinguished, comparable to the ones observed in Fig. 2c, i.e., smaller and curly vs. thicker and longer CNTs. A similar trend was also observed for samples prepared with $v = 55$ wt. %.

TEM measurements have been performed on selected samples in order to better characterize the morphology of the resulting materials. Figure 3 shows images of the materials produced with the following conditions: (a) $v = 37$ wt. % and $\varphi = 10$ sccm, (b) $v = 37$ wt. % and $\varphi = 35$ sccm, and (c) $v = 55$ wt. % and $\varphi = 10$ sccm. They demonstrate that the as-grown materials consist mainly of good quality MWNT, i.e., the tubes have smooth walls and few defects. Moreover, low amounts of by-products such as amorphous carbon or graphitic-like particles are detected. Ni particles and agglomerates can also be observed, some at the tip of the tubes, while others tubes present open tips. The TEM images also confirm that for large v the MWNT samples have a bimodal diameter distribution. They consist of a mixture of thicker, longer and straighter tubes (external and internal diameters: ~ 100 nm and ~ 20 nm, respectively), and thinner and more curly tubes (external diameter ~ 30 nm).

In order to further investigate the produced materials, XRD measurements were carried out. Figure 4 shows the XRD pattern of the material prepared with $v = 37$ wt. % and $\varphi = 10$ sccm. The diffraction peaks corresponding to Ni and YSZ are identified, and the NiO diffraction peaks are absent. The same features were also observed in all studied samples, demonstrating that the CVD process results in a complete reduction of the NiO particles. In addition, the XRD data were used to estimate the average crystallite size d_{Ni} of the resulting Ni nanoparticles. By using the Scherrer formula, d_{Ni} was determined to be ~ 36 nm and ~ 47 nm for the samples corresponding to $v = 37$ wt. % and 55 wt. %, respectively. The diffraction peak at $2\theta = 26°$ comes from the MWNT and correspond to the (002) planes of graphite. The interlayer spacing determined by the peak position is ~ 0.34 nm, which is a value close to the observed for MWNT [22].

Thermogravimetric analyses were also performed to provide a quantitative evaluation of the type and relative amounts of the carbonaceous species present in the as-grown mate-

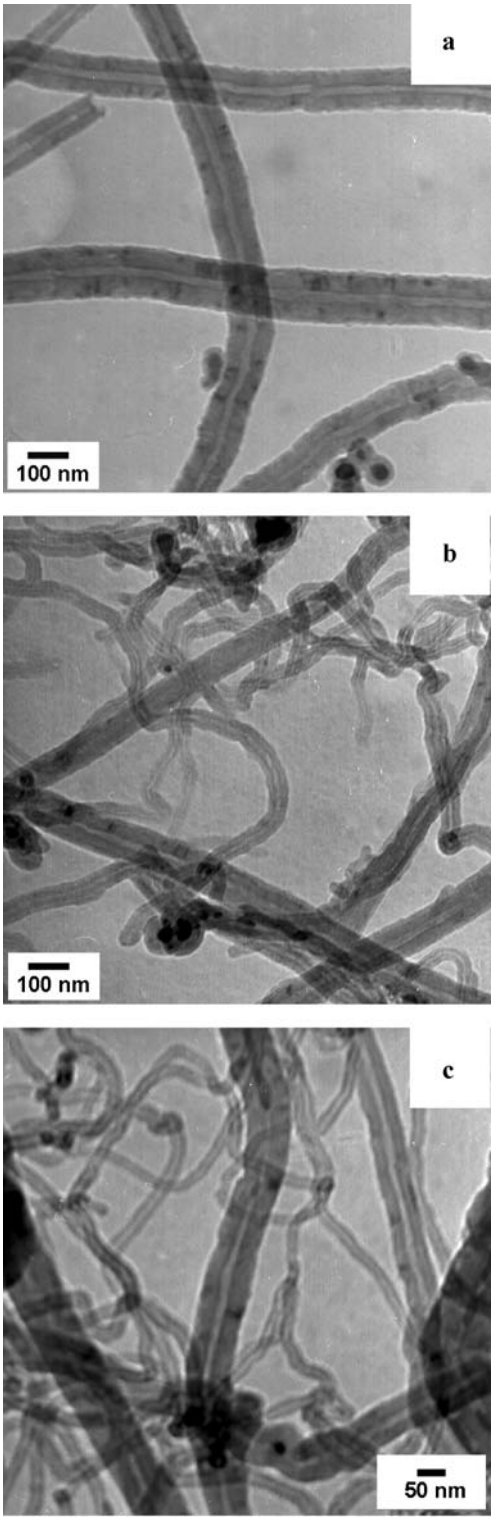

FIGURE 3 TEM images of the as-grown MWNT-materials prepared from catalysts with different Ni concentration (v), and by using different ethylene flux (φ): (**a**) $v = 37$ wt. %, $\varphi = 10$ sccm, (**b**) $v = 37$ wt. %, $\varphi = 35$ sccm, and (**c**) $v = 55$ wt. %, $\varphi = 10$ sccm

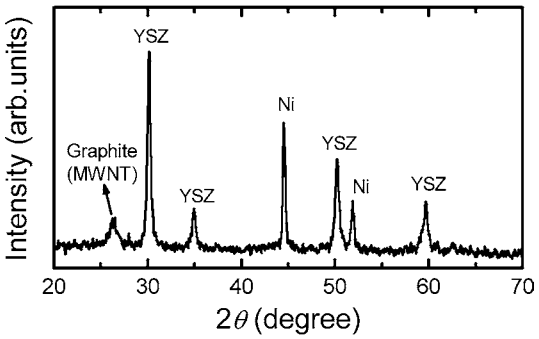

FIGURE 4 XRD pattern of the as-grown CNT-material prepared from catalysts with Ni concentration $v = 37$ wt. % and by using an ethylene flux of 10 sccm

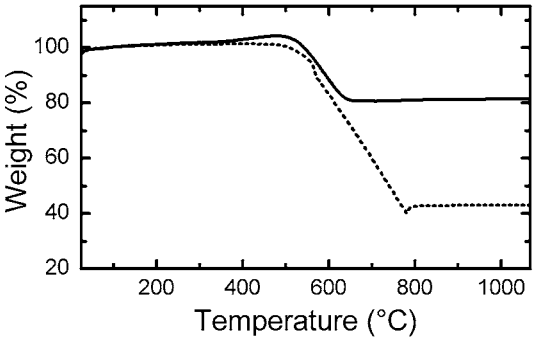

FIGURE 5 Thermogravimetric curves for the as-grown materials prepared from catalysts with Ni concentration, $v = 37$ wt. %, and by using ethylene fluxes, $\varphi = 10$ sccm (*solid lines*) and $\varphi = 35$ sccm (*dotted lines*)

rials. TGA has been widely applied to quantify the relative amounts of CNT, amorphous carbon, and catalyst materials (metals and/or ceramic supports) in CNT material produced by different techniques [22]. Figure 5 depicts TGA curves for the as-grown materials prepared with $v = 37$ wt. % and $\varphi = 10$ sccm (solid lines) and $\varphi = 35$ sccm (dotted lines). Upon heating, the first observed feature is a small weight gain ($\sim 5\%$–10%) in the 300–500 °C temperature range that can be attributed to the oxidation of the Ni particles. At ~ 500 °C, a pronounced weight loss starts to develop with increasing temperature as a result of the oxidation of the MWNT. Both the total weight loss and the temperature range in which it occurs are proportional to the MWNT content. The values for carbon content in the as-grown samples calculated by the TGA are similar to the ones obtained by weighing the catalyst powder before and after the MWNT growth, and correcting for the weight loss due to the reduction of the NiO, as inferred from the XRD data. These results suggest the complete removal of the MWNT for heat treatments above ~ 800 °C in oxidizing atmosphere. Furthermore, after the MWNT are fully decomposed, a slight but abrupt weight gain is observed for the material prepared with $\varphi = 35$ sccm. This weight gain at high temperature can be interpreted as being originated from the rapid oxidation of remaining Ni particles. Such metallic particles had been originally encapsulated inside the nanotubes and protected from oxidation. The TGA curves also indicate that no significant amorphous carbon was formed by the CVD process, since no noticeable weight loss is observed at temperatures lower than 400 °C. However, the weight loss due to the amorphous carbon could be hindered by the weight gain due to Ni oxidation in the same temperature range ($350\,°\text{C} < T < 500\,°\text{C}$). Nevertheless, the total weight gain associated with Ni oxidation is $\sim 5\%$ and $\sim 11\%$ for samples with $v = 37$ wt. % and 55 wt. % (not shown), respectively. These values are slightly lower than the expected nominal

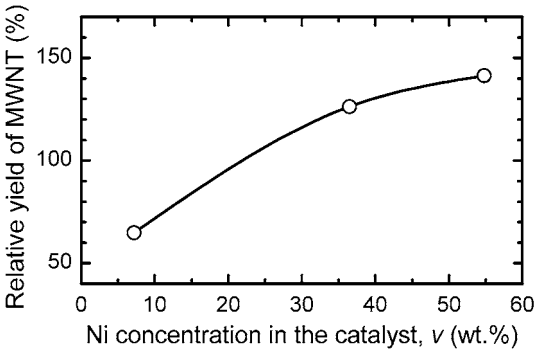

FIGURE 6 Dependence of the relative amount of MWNT on the Ni concentration (v) in the catalyst

ones ($\sim 9\%$ and 13%, respectively). Therefore, the relative amount of amorphous carbon present in the as-grown materials (if any) should be smaller than the difference between the expected and measured values ($\sim 4\%$). Similar TGA curves carried out under N_2 atmosphere revealed that no appreciable weight loss is observed up to 1100 °C, indicating that the MWNTs can be preserved if the YSZ/Ni/MWNT composites are heat treated at high temperatures in inert atmospheres.

Next, we discuss the effects of the Ni concentration in the catalysts on the MWNT growth. It is important to consider that the primary goal of the present work is to obtain a controlled growth of CNT from catalysts with a wide range of Ni concentration, rather than an optimized process for high yields. Figure 6 depicts the dependence of the process yield on the Ni concentration (v) in the catalyst. The yield is defined as the relative weight gain due to the CVD process after correcting for the weight loss in the catalyst powder due to the reduction of the NiO. Such values are representative of the relative content of MWNT in the as-grown materials as demonstrated by the TGA results of Fig. 5. For $v = 7$ wt. %, which is a value within the range commonly used for CNT growth, the yield is 65%. The yield roughly doubles when v is increased to 37 wt. % and then tends to saturate at $\sim 160\%$ for larger Ni concentrations. This is an unexpected and interesting result, since the utilization of catalysts with large metal concentration usually results in lower yields [24]. In addition, large amounts of amorphous carbon can also be formed in such cases. In this study, the relatively high yield observed is probably due to the good dispersion of NiO nanoparticles (5–10 nm) in the NiO/YSZ catalyst powder, even for large v (see Fig. 1). This characteristic can be related to the utilization of Ni acetate as the precursor in the catalyst powder preparation. Metal acetates have been shown to be more efficient metal precursors for the formation of very small catalyst cobalt nanoparticles (~ 2 nm) for single-wall CNT growth, if compared to other salts such as nitrates and sulfates [25]. The advantage of the metal acetate is attributed to its stronger interaction with the surface of the supporting oxide particles [26].

The properties of the catalyst powder are also responsible for the morphology of the resulting MWNT. The thinner and curly tubes observed in the SEM and TEM images of Figs. 2 and 3 have average diameters of ~ 30–40 nm, which are within the same range of the Ni crystallite size after the CVD process, as determined by the analysis of the XRD data (Fig. 4). This suggests that the MWNT diameter is controlled by the size of the Ni particles, in agreement with the most common accepted growth model, and as observed in several reports [1, 2]. On the other hand, the observed thicker (~ 100 nm) nanotubes obtained from catalysts with $v \geq 37$ wt. % are likely to originate from agglomerated Ni nanoparticles. From inspection of Fig. 1b, one can speculate that due to the large Ni content in the catalyst powder, part of the NiO nanoparticles are loosely anchored to the YSZ particles forming agglomerates. Therefore, upon heating and reduction during the H_2 pre-treatment, these agglomerates are likely to be converted to coarsened Ni particles/agglomerates.

4 Conclusion

Multi-walled carbon nanotubes were produced by chemical vapor deposition using (yttria-stabilized zirconia)/(nickel oxide) (YSZ/NiO) catalysts. The catalysts were synthesized by a liquid mixture technique that resulted in a fine dispersion of NiO nanoparticles embedded in the YSZ matrix. Two important results arise from this study: (i) dense YSZ particles can host high-weight fraction of metallic nanoparticles and lead to MWNT growth at relatively high-yields, with no significant amorphous carbon formation; (ii) composites, formed by the ionic conductor YSZ, the metallic Ni nanoparticles and the MWNT, having controlled composition and morphology can be produced by CVD by adjusting the process condition such as C_2H_4 flux and Ni concentration in the catalyst. The resulting as-grown YSZ/Ni/MWNT composites can be interesting due to the mixed ionic-electronic transport properties, which could be useful in electrochemical applications.

ACKNOWLEDGEMENTS This work was partially supported by the program "Instituto do Milênio de Nanociências" (MCT/CNPq). The authors are thankful to the Brazilian agencies FAPESP (DZF 03/08793-8, RM 99/10798-0) and CNPq (ASF 350601/2003-8 and 151555/2004-4, FCF 301.661/2004-9, RM 306.496/88), and the Italian Ministry of Education. Thanks are also due to N.M. Ferreira for the TEM measurements.

REFERENCES

1 M. Terrones, Ann. Rev. Mater. Res. **33**, 419 (2003)
2 Y. Ando, X. Zhao, T. Sugai, M. Kumar, Mater. Today **7**, 22 (2004)
3 H. Dai, A.G. Rinzler, P. Nikolaev, A. Thess, D.T. Colbert, R.E. Smalley, Chem. Phys. Lett. **260**, 471 (1996)
4 M. Terrones, N. Grobert, J. Olivares, J.P. Zhang, H. Terrones, K. Kordatos, W.K. Hsu, J.P. Hare, P.D. Townsend, K. Prassides, A.K. Cheetham, H.W. Kroto, D.R.M. Walton, Nature **388**, 52 (1997)
5 R. Sen, A. Govindaraj, C.N.R. Rao, Chem. Phys. Lett. **267**, 276 (1997)
6 P. Chen, H.B. Zhang, G.D. Lin, Q. Hong, K.R. Tsai, Carbon **35**, 1495 (1997)
7 J. Kong, A.M. Cassell, H. Dai, Chem. Phys. Lett. **292**, 567 (1998)
8 A. Cassell, J.A. Raymakers, J. Kong, H. Dai, J. Phys. Chem. B **103**, 6484 (1999)
9 K. Mukhopadhyay, A. Koshio, T. Sugai, N. Tanaka, H. Shinohara, Z. Konya, J.B. Nagy, Chem. Phys. Lett. **303**, 117 (1999)
10 J.F. Colomer, C. Stephan, S. Lefrant, G. Van Tendeloo, I. Willems, Z. Konya, Chem. Phys. Lett. **317**, 83 (2000)
11 A.-C. Dupuis, Prog. Mater. Sci. **50**, 929 (2005)
12 C. Laurent, A. Peigney, O. Dumortier, A. Rousset, J. Eur. Ceram. Soc. **18**, 2005 (1998)
13 V. Esposito, C. D'Ottavi, S. Ferrari, S. Licoccia, E. Traversa, In *Solid Oxide Fuel Cells VIII – Proceedings of the 8th International Symposium*, ed. by S.C. Singhal, M. Dokiya (The Electrochemical Society Inc., New York, 2002), p. 643–654

14 V. Esposito, D.Z. de Florio, F.C. Fonseca, E.N.S. Muccillo, R. Muccillo, E. Traversa, J. Eur. Ceram. Soc. **25**, 2637 (2005)
15 N.M. Minh, Solid State Ionics **174**, 271 (2004)
16 B.C.H. Steele, J. Mater. Sci. **36**, 1053 (2001)
17 S. Kurasawa, S. Iwamoto, M. Inoue, Mol. Cryst. Liq. Cryst. **387**, 347 (2002)
18 Y. Nagayasu, A. Nakayama, S. Kurasawa, S. Iwamoto, E. Yagasaki, M. Inoue, J. Jpn. Petrol. Inst. **48**, 301 (2005)
19 S.J. Han, T.K. Yu, J. Park, B. Koo, J. Joo, T. Hyeon, S. Hong, J. Im, J. Phys. Chem. B **108**, 8091 (2004)
20 T. Takeguchi, S. Furukawa, M. Inoue, J. Catal. **202**, 14 (2001)
21 D.W. Dees, T.D. Claar, T.E. Easler, D.C. Fee, F.C. Mrazek, J. Electrochem. Soc. **134**, 2141 (1987)
22 R. Andrews, D. Jacques, D. Qian, E.C. Dickey, Carbon **39**, 1681 (2001)
23 L.S.K. Pang, J.D. Saxby, S.P. Chatfield, J. Phys. Chem. **97**, 6941 (1993)
24 M. Perez-Cabero, I. Rodriguez-Ramos, A. Guerrero-Ruiz, J. Catal. **215**, 305 (2003)
25 Y. Murakami, S. Chiashi, Y. Miyauchi, S. Maruyama, Jpn. J. Appl. Phys. **43**, 1221 (2004)
26 S. Sun, N. Tsubaki, K. Fujimoto, Appl. Catal. A **202**, 121 (2000)